

Large surface enhanced Raman scattering enhancements from fracture surfaces of nanoporous gold

L. H. Qian, A. Inoue, and M. W. Chen

Citation: [Applied Physics Letters](#) **92**, 093113 (2008); doi: 10.1063/1.2890164

View online: <http://dx.doi.org/10.1063/1.2890164>

View Table of Contents: <http://scitation.aip.org/content/aip/journal/apl/92/9?ver=pdfcov>

Published by the [AIP Publishing](#)

Articles you may be interested in

[Recyclable surface-enhanced Raman scattering template based on nanoporous gold film/Si nanowire arrays](#)
Appl. Phys. Lett. **105**, 011905 (2014); 10.1063/1.4889850

[ZnO/Si arrays decorated by Au nanoparticles for surface-enhanced Raman scattering study](#)
J. Appl. Phys. **111**, 033104 (2012); 10.1063/1.3682462

[Geometric effect on surface enhanced Raman scattering of nanoporous gold: Improving Raman scattering by tailoring ligament and nanopore ratios](#)
Appl. Phys. Lett. **94**, 213109 (2009); 10.1063/1.3143628

[Surface enhanced Raman scattering of nanoporous gold: Smaller pore sizes stronger enhancements](#)
Appl. Phys. Lett. **90**, 153120 (2007); 10.1063/1.2722199

[Surface-enhanced Raman scattering on nanoporous Au](#)
Appl. Phys. Lett. **89**, 053102 (2006); 10.1063/1.2260828

The advertisement features a 3D cutaway illustration of a mechanical part with a red and yellow stress field. The text 'Over 600 Multiphysics Simulation Projects' is prominently displayed in white and blue. A blue button with the text 'VIEW NOW >>' is located in the bottom right corner. The COMSOL logo is positioned at the bottom right of the image.

Over **600** Multiphysics
Simulation Projects

[VIEW NOW >>](#)

COMSOL

Large surface enhanced Raman scattering enhancements from fracture surfaces of nanoporous gold

L. H. Qian, A. Inoue, and M. W. Chen^{a)}

Institute for Materials Research and WPI Advanced Institute for Materials Research, Tohoku University, Sendai 980-8577, Japan

(Received 29 December 2007; accepted 11 February 2008; published online 5 March 2008)

We report the improved surface enhanced Raman scattering (SERS) of mechanically ruptured nanoporous gold. The SERS intensities of rhodamine 6G and crystal violet 10B molecules from the fracture surfaces of nanoporous gold are about one order of magnitude higher than those from the as-prepared samples. Microstructural characterization reveals that the fracture surfaces contain numerous sharp protrusions with 5–10 nm apexes, produced by localized plastic deformation of gold ligaments during failure. The large SERS enhancements from the fracture surfaces are most likely associated with the intensified electromagnetic fields around the nanosized protrusions and the electromagnetic interaction between the protrusions.

© 2008 American Institute of Physics. [DOI: 10.1063/1.2890164]

Surface enhanced Raman scattering (SERS) arising from nanostructured noble metals is a promising technique for molecular detections and diagnoses because of the significantly improved Raman intensity of organic molecules and the precise identification of molecular structures.^{1–3} It has been found that the SERS enhancements remarkably rely on the size, shape, and assembly of metallic nanostructures.^{4–10} Many efforts have been made to exploit nanostructured metals as ultrasensitive SERS substrates by microstructure optimizations.^{11–16} Among various nanostructured metals, bicontinuous nanoporous gold with tunable nanoporosity has recently been developed as a promising SERS substrate by optimizing their nanoporosity.^{17–19} Large SERS enhancements have been achieved from ultrafine nanoporous gold prepared by low-temperature dealloying and from coarsened gold ligaments with nanosized surface “pimples” by high-temperature annealing.^{17,19,20} However, the underlying mechanisms on the SERS effects of nanoporous gold remain unclear. In this letter, we report largely improved SERS enhancements from mechanically ruptured surfaces of nanoporous gold, which paves a new way to improve the SERS effects of nanoporous gold and is helpful to understand the SERS mechanisms of nanoporous gold.

Ag₆₅Au₃₅ (at. %) sheets with a thickness of $\sim 100 \mu\text{m}$ were used for fabricating nanoporous gold. Selective dissolution of silver atoms in 70% (mass ratio) HNO₃ aqueous solution at room temperature for 48 h leads to the formation of bicontinuous nanoporosity across the entire sheets. A nanoporous gold sheet was first placed on a glass slide and then partly covered by an aluminum cube with smooth and straight edges. The side length of the cube (20 mm) is much larger than the width of nanoporous gold sheet ($\sim 5 \text{ mm}$) and the entire nanoporous sheet was sliced along an edge of the aluminum cube by a sharp knife. To make smooth cutting surfaces, the sharp edge of the knife is vertical to the surface of nanoporous gold sheet during cutting. The overall roughness of the cutting surfaces is smaller than submicron, which can ensure the reproducible acquisition of Raman scattering from the ruptured surfaces. Even the knife is very sharp, its

edge is still about micrometer-scale thick, which is much larger than the nanosized gold ligaments. Thus, the failure of each ligament is mainly by pulling and/or bending, resulting in sharp tips of fractured ligaments. The ruptured surfaces were placed faceup for SERS measurements. Two types of molecules, rhodamine 6G (R6G) and crystal violet (CV) 10B, were used to examine the SERS properties of the as etched and fractured nanoporous gold. The detailed process of the SERS experiments has been reported before.¹⁹ Scanning electron microscope (SEM) and transmission electron microscope (TEM) observations were conducted to characterize the microstructure of the fracture surfaces and the as-prepared samples.

Representative SEM image, as shown in Fig. 1(a), illustrates the microstructure of the as-prepared nanoporous gold with open nanoporosity in three dimensions. Statistical analysis by a rotational fast Fourier transform method²¹ sug-

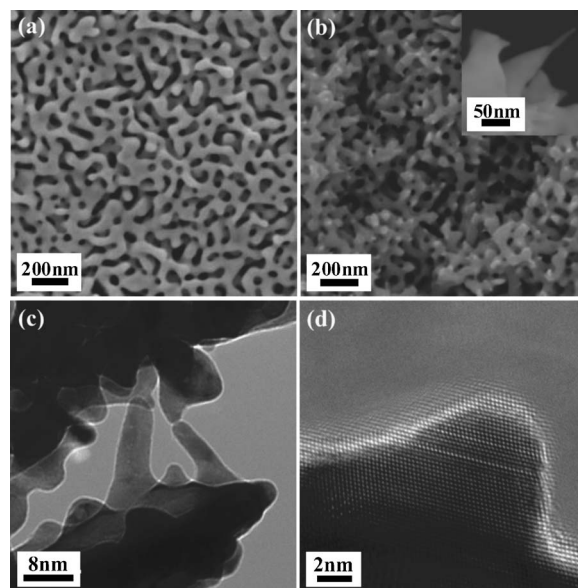


FIG. 1. (a) SEM micrograph of as-prepared nanoporous gold and (b) the fracture surface of nanoporous gold. The inset shows the morphology of the fractured ligaments with sharp tips. (c) Bright-field TEM image of fractured gold ligaments and (d) HREM image of the nanosized apex of a fractured ligament. Deformation twins and stacking faults are frequently observed in the fractured ligaments.

^{a)} Author to whom correspondence should be addressed. Electronic mail: mwchen@imr.tohoku.ac.jp

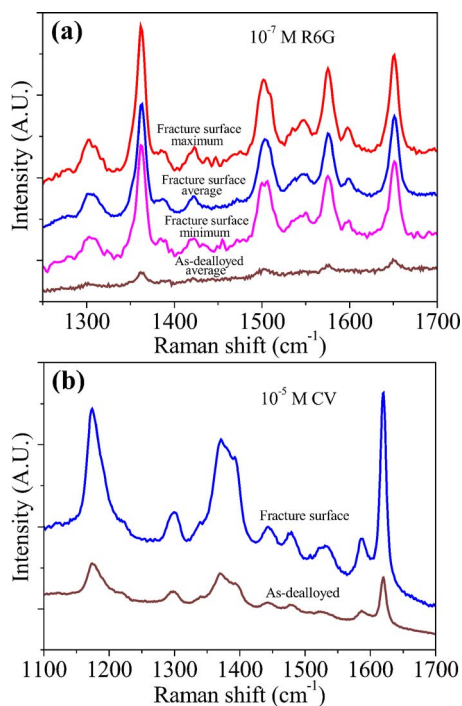


FIG. 2. (Color online) Representative SERS spectra of organic molecules absorbed onto the as-prepared and fractured nanoporous gold surfaces. (a) 10^{-7} mol/l R6G molecules detected by 514.5 nm laser and (b) 10^{-5} mol/l CV molecules detected by 632.8 nm laser.

gests that the characteristic length scale of the as-prepared sample is ~ 60 nm in diameter for both nanopores and gold ligaments. A fracture surface of nanoporous gold is shown in Fig. 1(b), from which detectable change in the nanopore size cannot be identified. However, a large number of protrusions as the result of broken gold ligaments appear on the fracture surfaces with a bright contrast [Fig. 1(b)]. The spear-shaped protrusions generally have sharp tips [the inset of Figs. 1(b) and 1(c)], which are much smaller than the original ligament diameter of ~ 60 nm. High-resolution electron microscopy (HREM) of the protrusions reveals that the apexes have a diameter of 5–10 nm [for an example, Fig. 1(d)]. Deformation defects, such as deformation twins and stacking faults, can be frequently observed in the broken gold ligaments, indicating the formation of the sharp tips are associated with the localized plastic deformation of gold ligaments during failure.²²

The SERS spectra of R6G molecules on as-prepared nanoporous gold are shown in Fig. 2(a). Raman bands corresponding to the characteristic vibrational modes of R6G molecules can be observed.^{19,23} However, the scattering intensities are very weak and only major bands can be detected. Dramatic improvement in the Raman scattering is achieved from the fracture surfaces of nanoporous gold. With the same experimental conditions, the intensities of the R6G Raman bands are approximately ten times higher than those from the as-prepared nanoporous gold. Moreover, the minor SERS bands of R6G molecules that are too weak to be detected from the as-prepared nanoporous gold can be well identified from the fracture surfaces. Although the fracture surfaces are not flat at the submicron scale, as shown by the SEM image [Fig. 1(b)], the SERS intensities of R6G molecules from various regions do not change too much [Fig. 2(a)], indicating the microstructure of the fracture surfaces is relatively homogeneous.

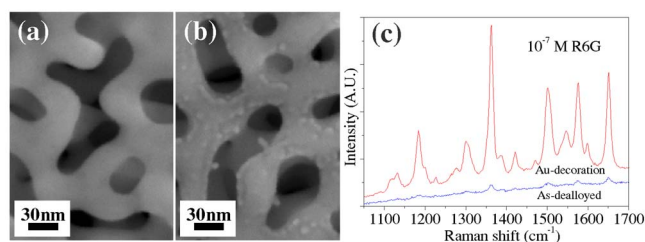


FIG. 3. (Color online) (a) SEM micrograph of as-prepared nanoporous gold, (b) surface morphology of nanoporous gold with the deposited gold nanoparticles, and (c) the corresponding SERS spectra of 10^{-7} mol/l R6G molecules from the as-prepared nanoporous gold (a) and the deposited sample (b) detected by 514.5 nm laser.

To demonstrate that the improved SERS effects of R6G from the fracture surfaces is an intrinsic phenomenon arising from the microstructure of ruptured nanoporous gold, another organic reagent, CV 10B, is also used as the test probe. Figure 2(b) illustrates the SERS spectra of 10^{-5} mol/l CV molecules from the as-prepared and fractured nanoporous gold. The analogous improvements can be observed, i.e., the SERS enhancement from the mechanically ruptured surfaces is about five times higher than that from the as-prepared nanoporous gold with the exactly same acquisition parameters. The slightly lower improvement than that of the R6G molecules [about ten times, as shown in Fig. 2(a)] is probably related to their diversities in the distinct absorption behaviors on gold surfaces and in the intrinsic enhancement factors from gold substrates.

According to the SEM and TEM micrographs, the distinct difference between the as-prepared and the ruptured nanoporous gold is the appearance of the sharp protrusions on the fracture surfaces. Thus, the improved SERS enhancements from the fracture surfaces are most likely associated with the nanosized protrusions on the top surfaces. To confirm this supposition, gold nanoparticles were deposited onto the as-prepared nanoporous gold surfaces by physical vapor deposition with high purity gold as a sputtering target. Figures 3(a) and 3(b) show the morphological changes of the nanoporous gold surfaces before and after the deposition. By optimizing sputtering conditions, the top surface of the deposited nanoporous gold is decorated by gold nanoparticles in the form of nanosized protrusions, similar to the fracture surfaces. The size of the deposited gold nanoparticles, 5–10 nm, is fairly comparable to the diameters of the protrusion apexes in the ruptured surfaces [Fig. 1(b)]. Figure 3(c) represents the Raman spectra of R6G molecules from the nanoporous gold substrates with and without the deposited gold nanoparticles. The analogous improvement in the SERS enhancement is achieved from the nanoporous gold with the decorated nanoparticles, which is also about one order of magnitude higher than that from the as-prepared porous gold. Therefore, we can conclude that the dramatically improved SERS effects from the fractured nanoporous gold surfaces originate from the nanosized protrusions produced by the broken gold ligaments.

A number of experiments and simulations have demonstrated that the localized electromagnetic fields play important roles in the improved SERS effects^{24–28} and steep edges of sharp protrusions can offer an additional enhancement in comparison with the blunt edges.²⁸ Accordingly, our observations of the largely improved SERS enhancements from the fractured surfaces apparently result from a large number

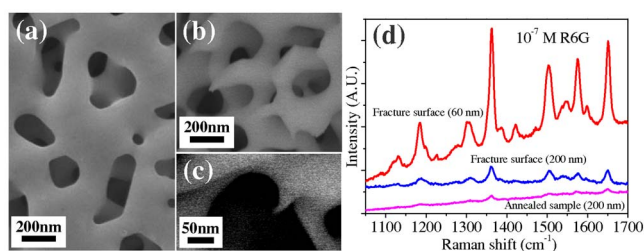


FIG. 4. (Color online) (a) SEM micrograph of nanoporous gold annealed at 300 °C for 2 h, (b) the fracture surface of the coarsened nanoporous gold, (c) the sharp tip of a fractured ligament, and (d) the corresponding SERS spectra of 10^{-7} mol/l R6G molecules from annealed nanoporous gold and the fracture surfaces detected by 514.5 nm laser.

of the sharp protrusions produced by localized deformation of gold ligaments during mechanical failure. The fractured gold ligaments with sharp tips can provide intensified electromagnetic fields around the nanosized apices.²⁸ Although the electromagnetic enhancements are localized around the apex of each protrusion, a large number of ruptured ligaments with a high density on the fracture surfaces result in a macroscopic effect for the overall improvements in SERS enhancements.

In addition to the localized electromagnetic effect arising from individual protrusions, electromagnetic coupling among the sharp tips with distance smaller than 10 nm may also play an important role in the improved SERS enhancements of ruptured nanoporous gold.¹⁵ To clarify the possible coupling effect, we change the average interprotrusion distance by cutting a coarsened nanoporous gold sample that was prepared by annealing the as-dealloyed sample at 300 °C for 2 h.¹⁹ Figure 4(a) is the SEM micrograph of the annealed nanoporous gold. The average size of nanopores and ligaments is ~ 200 nm, which is about three to four times larger than that of the as-dealloyed samples. The ruptured ligaments on the fracture surface also have 5–10 nm sharp tips but the density of the protrusions ($5/\mu\text{m}^2$) is about three to four times lower than that ($15\sim 20/\mu\text{m}^2$) on the fracture surface of the as-prepared nanoporous gold [Figs. 4(b) and 4(c)]. The interprotrusion distance is generally larger than 100 nm and, in principle, the electromagnetic interaction between the fractured ligaments should not be significant. The SERS measurements reveal the SERS enhancements of the fracture surfaces of the coarsened nanoporous gold is about three times higher than that of the annealed sample [Fig. 4(d)], further confirming that the fractured ligaments with a sharp tip can dramatically improve the SERS effect of nanoporous gold. However, in comparison with the SERS improvement of the fractured surfaces of the 60 nm nanoporous gold, the enhancement factor of the fracture surfaces of the 200 nm sample is about 6–7 times smaller. Even considering the density difference (about three to four times difference) of the ruptured ligaments on the fracture surfaces of the two samples, one can find that there is still 2–4 times disparity in the SERS enhancement factors. Apparently, in addition to the localized electromagnetic effect arising from the sharp apex of individual fractured gold ligaments, the electromagnetic coupling among the neighboring fractured ligaments plays an important role in the large SERS enhancements of the fracture surfaces of nanoporous gold with a small pore size.

In general, the SERS effects of nanoporous gold have been attributed to possible chemical enhancements from

large internal surface areas for molecular adsorptions and electromagnetic enhancements from the localized surface plasmon resonance. Additionally, both gold ligaments with a positive curvature and nanopores with a negative curvature are possible origins of the intensified surface plasmon resonance. According to the present observations, the dramatic improvements from the fractured surfaces strongly suggest that the chemical contribution in the SERS effects of nanoporous gold is minor and the dominant enhancements come from the top surface layers with intensified surface plasmon resonance and coupling. The gold ligaments with positive curvatures appear to play a prevailing role in SERS effects of nanoporous gold, rather than nanopores with negative curvatures. It is interesting to note that the enhancement factor of the fractures surfaces is very close to that of ultrafine nanoporous gold with the nanopore and ligament sizes of about 5–10 nm.¹⁹ Thus, the improved SERS enhancements with reducing nanopore sizes, observed previously, most likely result from the enhanced electromagnetic effect from small gold ligaments.

- ¹M. Moskovits, *Rev. Mod. Phys.* **57**, 783 (1985).
- ²K. Kneipp, H. Kneipp, I. Itzkan, R. R. Dasari, and M. S. Feld, *Chem. Rev. (Washington, D.C.)* **99**, 2957 (1999).
- ³C. J. Murphy, T. K. San, A. M. Gole, C. J. Orendorff, J. X. Gao, L. Gou, S. E. Hunyadi, and T. Li, *J. Phys. Chem. B* **109**, 13857 (2005).
- ⁴U. Kreibig and L. Genzel, *Surf. Sci.* **156**, 678 (1985).
- ⁵S. Link and M. A. El-Sayed, *J. Phys. Chem. B* **103**, 8410 (1999).
- ⁶P. M. Tessier, O. D. Velev, A. T. Kalambur, J. F. Rabolt, A. M. Lenhoff, and E. W. Kaler, *J. Am. Chem. Soc.* **122**, 9554 (2000).
- ⁷A. Tao, F. Kim, C. Hess, J. Goldberger, R. R. He, Y. G. Sun, Y. N. Xia, and P. D. Yang, *Nano Lett.* **3**, 1229 (2003).
- ⁸E. Hao and G. C. Schatz, *J. Chem. Phys.* **120**, 357 (2004).
- ⁹Y. J. Xiong, J. M. McLellan, J. Y. Chen, Y. D. Yin, Z. Y. Li, and Y. N. Xia, *J. Am. Chem. Soc.* **127**, 17118 (2005).
- ¹⁰C. H. Sun, N. C. Linn, and P. Jiang, *Chem. Mater.* **19**, 4551 (2007).
- ¹¹L. H. Lu, R. Capek, A. Kornowski, N. Gaponik, and A. Eychmuller, *Angew. Chem.* **44**, 5997 (2005).
- ¹²H. Wang, C. S. Levin, and N. J. Halas, *J. Am. Chem. Soc.* **127**, 14992 (2005).
- ¹³B. N. J. Persson, K. Zhao, and Z. Y. Zhang, *Phys. Rev. Lett.* **96**, 207401 (2006).
- ¹⁴X. Y. Zhang, J. Zhao, A. V. Whitney, J. W. Elam, and R. P. Van Duyne, *J. Am. Chem. Soc.* **128**, 10304 (2006).
- ¹⁵H. H. Wang, C. Y. Liu, S. B. Wu, N. W. Liu, C. Y. Peng, T. H. Chan, C. F. Hsu, J. K. Wang, and Y. L. Wang, *Adv. Mater. (Weinheim, Ger.)* **18**, 491 (2006).
- ¹⁶H. X. Xu, J. Aizpurua, M. Kall, and P. Apell, *Phys. Rev. E* **62**, 4318 (2000).
- ¹⁷S. O. Kucheyev, J. R. Hayes, J. Biener, T. Huser, C. E. Talley, and A. V. Hamza, *Appl. Phys. Lett.* **89**, 53102 (2006).
- ¹⁸M. C. Dixon, T. A. Daniel, M. Hieda, D. M. Smligies, M. H. W. Chan, and D. L. Allara, *Langmuir* **23**, 2414 (2007).
- ¹⁹L. H. Qian, X. Q. Yan, T. Fujita, A. Inoue, and M. W. Chen, *Appl. Phys. Lett.* **90**, 153120 (2007).
- ²⁰L. H. Qian and M. W. Chen, *Appl. Phys. Lett.* **91**, 83105 (2007).
- ²¹T. Fujita and M. W. Chen, *Jpn. J. Appl. Phys.* **47**, 1161 (2008).
- ²²J. Biener, A. M. Hodge, and A. V. Hamza, *Appl. Phys. Lett.* **87**, 121908 (2005).
- ²³P. Hildebrandt and M. Stockburger, *J. Phys. Chem.* **88**, 5935 (1984).
- ²⁴B. Pettinger, B. Ren, G. Picardi, R. Schuster, and G. Ertl, *Phys. Rev. Lett.* **92**, 96101 (2004).
- ²⁵C. E. Talley, J. B. Jackson, C. Oubre, N. K. Grady, C. W. Hollars, S. M. Lane, T. R. Huser, P. Nordlander, and N. J. Halas, *Nano Lett.* **5**, 1569 (2005).
- ²⁶D. D. Evanoff and G. Chumanov, *ChemPhysChem* **6**, 1221 (2005).
- ²⁷F. Jackel, A. A. Kinkhabwala, and W. E. Moerner, *Chem. Phys. Lett.* **446**, 339 (2007).
- ²⁸W. H. Zhang, X. D. Cui, B. S. Yeo, T. Schmid, C. Hafner, and R. Zenobi, *Nano Lett.* **7**, 1401 (2007).